

LD CAEN

LABORATOIRE DE PHYSIQUE CORPUSCULAIRE

ISMRA - Boulevard Maréchal Juin - 14050 CAEN CEDEX - FRANCE

CERN LIBRARIES, GENEVA

SCAN-9706065



APPARENT TEMPERATURES IN HOT QUASI-PROJECTILES  
AND THE CALORIC CURVE

J. Péter, M. Assenard, F. Gulminelli, Ma Y.-G., A. Siwek,  
and INDRA Collaboration

Sw 97 24

March 1997

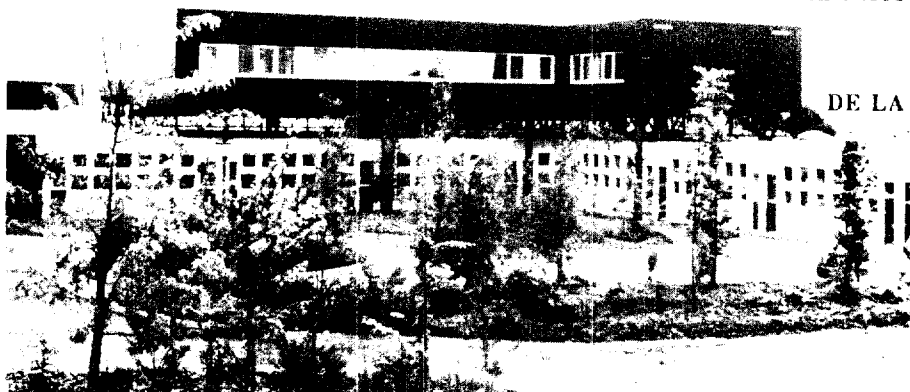
LPCC 97-08  
SUBATECH 97-08  
LYCEN 9711  
IPNO-DRE 97-12  
DAPNIA/SPhN 97-19  
GANIL P 9709

Presented at 13 th Winter Workshop Meeting on Nuclear  
Dynamics, Marathon, Florida, USA, 1-7, February 1997

INSTITUT NATIONAL  
DE PHYSIQUE NUCLEAIRE ET DE PHYSIQUE DES PARTICULES  
CENTRE NATIONAL DE LA RECHERCHE SCIENTIFIQUE

INSTITUT DES SCIENCES  
DE LA MATIERE ET DU RAYONNEMENT

Téléphone : 02 31 45 25 00  
Télécopie : 02 31 45 25 49



## APPARENT TEMPERATURES IN HOT QUASI-PROJECTILES AND THE CALORIC CURVE.

J. Péter<sup>1</sup>, M. Assenard<sup>5</sup>, F. Gulminelli<sup>1</sup>, Ma Y.-G.<sup>1</sup>, A. Siwek<sup>1</sup>, G. Auger<sup>2</sup>, Ch.O. Bacri<sup>6</sup>, J. Benlliure<sup>3</sup>, E. Bisquer<sup>4</sup>, F. Bocage<sup>1</sup>, B. Borderie<sup>6</sup>, R. Bougault<sup>1</sup>, R. Brou<sup>1</sup>, P. Buchet<sup>2</sup>, J.L. Charvet<sup>2</sup>, A. Chbihi<sup>3</sup>, J. Colin<sup>1</sup>, D. Cussol<sup>1</sup>, R. Dayras<sup>2</sup>, E. De Filippo<sup>2</sup>, A. Demeyer<sup>4</sup>, D. Doré<sup>6</sup>, D. Durand<sup>1</sup>, P. Eudes<sup>5</sup>, J. D. Frankland<sup>6</sup>, E. Galichet<sup>4</sup>, E. Genouin-Duhamel<sup>1</sup>, E. Gerlic<sup>4</sup>, M. Germain<sup>5</sup>, D. Gourio<sup>5</sup>, D. Guinet<sup>4</sup>, P. Lantesse<sup>4</sup>, J.L. Laville<sup>5</sup>, J.F. Lecomte<sup>1</sup>, A. Le Fèvre<sup>3</sup>, T. Lefort<sup>1</sup>, R. Legrain<sup>2</sup>, O. Lopez<sup>1</sup>, M. Louvel<sup>1</sup>, N. Marie<sup>3</sup>, V. Métivier<sup>5</sup>, L. Nalpas<sup>2</sup>, A. D. Nguyen<sup>1</sup>, M. Parlog<sup>8</sup>, E. Plagnol<sup>6</sup>, O. Politi<sup>3</sup>, A. Rahmani<sup>5</sup>, T. Reposeur<sup>5</sup>, M.F. Rivet<sup>6</sup>, E. Rosato<sup>7</sup>, F. Saint-Laurent<sup>3</sup>, S. Salou<sup>3</sup>, J.C. Steckmeyer<sup>1</sup>, M. Stern<sup>4</sup>, G. Tabacaru<sup>8</sup>, B. Tamain<sup>1</sup>, L. Tassan-Got<sup>6</sup>, O. Tittel<sup>3</sup>, E. Vient<sup>1</sup>, C. Volant<sup>2</sup>, J.P. Wieleczko<sup>3</sup>

<sup>1</sup>L.P.C. Caen (IN2P3-CNRS/ISMRA et Université), Caen, France

<sup>2</sup>C.E.A. DAPNIA-SPhN, C.E. Saclay, France

<sup>3</sup>GANIL (DSM-CEA/IN2P3-CNRS), Caen, France

<sup>4</sup>I.P.N. Lyon (IN2P3-CNRS/Université), Villeurbanne, France

<sup>5</sup>SUBATECH (IN2P3-CNRS/Université), Nantes, France

<sup>6</sup>I.P.N. Orsay (IN2P3-CNRS), Orsay, France

<sup>7</sup>Dipartimento di Scienze, Univ. di Napoli, Italy

<sup>8</sup>I.F.I.N., I.F.A., Bucharest, Romania.

## INTRODUCTION

The dependence of nuclear temperature upon excitation energy has been experimentally studied with increasing values of excitation energy over the years. At excitation energies per nucleon,  $E^*/A$ , lower than 6 MeV the temperatures deduced from the kinetic properties of the emitted particles and clusters follow the Fermi gas law :  $E^* = (A/k).T^2$ . The value of the inverse level density parameter  $k$  was found to be in the range 8 to 13<sup>[1]</sup>. When excitation energies up to 10 MeV per nucleon were reached, temperatures obtained from the relative populations of excited levels in the emitted light nuclei did not overcome 5-6 MeV <sup>[2]</sup>, but this limitation could be explained by side-feeding effects. Such hot nuclei were formed in fusion or deep inelastic reactions. At incident energies above 40-50 MeV/u, binary dissipative collisions dominate and the quasi-projectiles reach excitation energies per nucleon and kinetic temperatures above 10 MeV<sup>[4, 5]</sup>. The study of projectile "spectators" in reactions at several

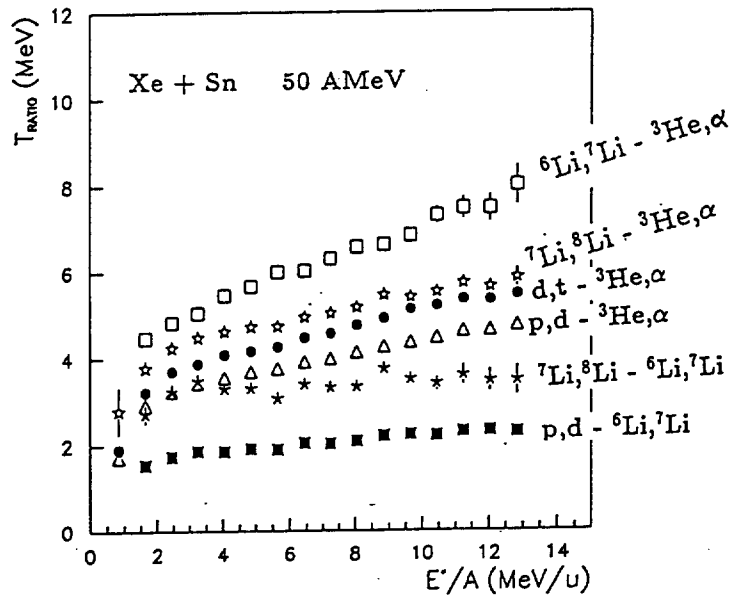


Figure 1. Measured apparent temperature obtained from double isotopic yield ratios versus excitation energy per nucleon of quasi-projectiles with masses  $1115 \pm 20\%$  formed in  $^{129}\text{Xe}$  collisions on Sn at 50 A MeV.

hundreds of MeV/u made it possible to reach similar excitation energies [3]. In this Aladin experiment at GSI, the temperature was obtained via the relative abundances of two isotope pairs [6]. The relation between this temperature  $Tr^0$  and  $E^*/A$  was interpreted as indicating a phase transition, with the nuclear gas regime dominating above  $E^*/A = 10$  MeV, as predicted [7]. However, a monotonic increase of the temperature with excitation energy was observed in similar conditions [8] and questions were raised about the significance of these caloric curves [9, 10, 11, 12], about the role played by the mass dependence of the decaying nucleus upon  $E^*/A$  [13], as well as the strong effects of side-feeding, especially at high temperatures [14]. This point will be discussed by Xi Hong Fei at this meeting. [15].

With Indra at GANIL, the temperature-excitation energy relationship was studied for  $E^*$  ranging from 2 to 24 MeV per nucleon in the quasi-projectiles issued from the reaction  $^{36}\text{Ar} + ^{58}\text{Ni}$  at 95 MeV/u. Different prescriptions for the determination of temperatures were applied and compared: apparent temperatures extracted from several pairs of isotopes and from the slopes of light charged particle kinetic energy spectra. No indication was found for a fast phase transition [16]. In this paper we show in addition temperatures determined from the population of excited discrete levels, as well as results obtained at 52 and 74 MeV/u and for quasi-projectiles from the reaction  $^{129}\text{Xe} + ^{124}\text{Sn}$  at 50 MeV/u. The strong role played by successive de-excitation steps and side-feeding is studied within two very different scenarios.

## EXPERIMENTS

The kinetic energies of charged products were measured with the  $4\pi$  detector array INDRA covering 90% of the  $4\pi$  solid angle. Isotopic separation was achieved for elements up to  $Z=4$ .

As for heavier and lighter systems having the same mass asymmetry studied previously at neighbouring incident energies [4, 5], the dominant process is the formation of a quasi-projectile (QP) and a quasi-target (QT) accompanied by dynamical emission around mid-

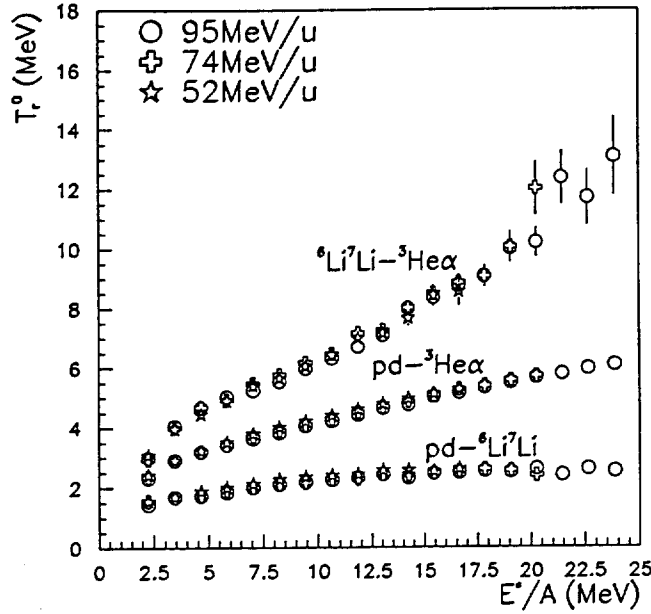


Figure 2. Same as Fig.1 for quasi-projectiles with masses  $33 \pm 20\%$  formed in  $^{36}\text{Ar}$  collisions on Ni at 52, 74 and 95 A MeV.

rapidity. All QP products have velocities well above the detection and isotopic separation thresholds. Therefore, the QP was reconstructed as in [5]. To avoid mass dependence effects, QP's with equal masses (within  $\pm 20\%$ ) were selected.

Determining a temperature value is justified only if thermal equilibrium was achieved in the source. Experimentally one can check that the angular distributions of various products are isotropic in the source frame (or forward-backward symmetric if the source has a large spin). This is not sufficient to establish that equilibrium had been attained, but this is a necessary condition. The QP products, ranging from protons to  $^8\text{Li}$ , fulfill this condition at all impact parameters.

The QP excitation energy is equal to the mass balance between the QP mass and its products, added to the sum of kinetic energies of its products in its frame. The kinetic energy of neutrons was taken as the average kinetic energy of protons in the same impact parameter bin, corrected for the absence of Coulomb barrier. Due to large fluctuations in the energy sharing between QP and QT, the excitation energy per nucleon reaches values above the available energy per nucleon in central collisions, as already seen for this system [17]. Details can be found in [16].

## APPARENT TEMPERATURES FROM ISOTOPIC RATIOS

Temperatures were calculated from the yields  $Y$  of several pairs of light isotopes differing by one neutron, according to [6]:

$$Tr_{n-d}^0 = B / \ln \left( a \cdot \frac{Y(Z_n, A_n) / Y(Z_n, A_n + 1)}{Y(Z_d, A_d) / Y(Z_d, A_d + 1)} \right) \quad (2)$$

where  $n$  ( $d$ ) stands for the pair of isotopes with the smallest (largest) binding energy difference, and appears at the numerator (denominator).

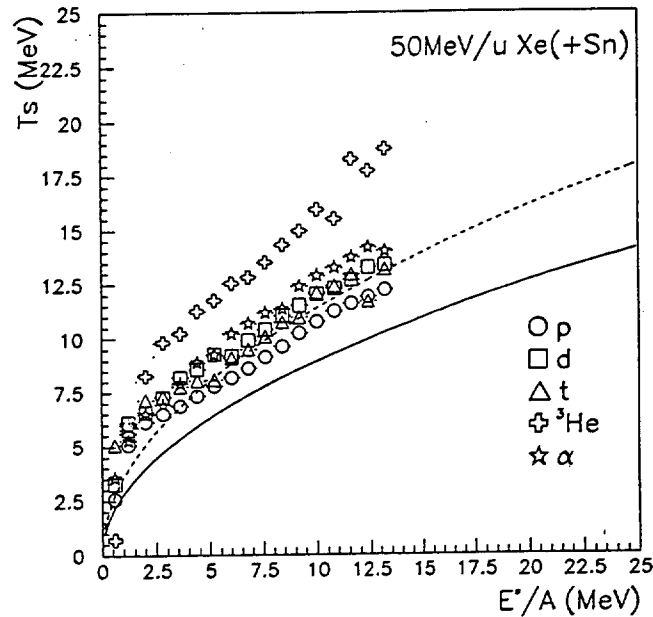


**Figure 3.** Measured slope parameters from kinetic energy spectra for light particles emitted by quasi-projectiles formed in  $^{129}\text{Xe}$  collisions on Sn at 50 A MeV. For orientation, the Fermi gas relationship is shown with  $A/8$  (solid line) and  $A/12$  (dashed line).

By choosing isotopes which do not have low lying levels decaying via  $\gamma$  emission, one can calculate  $a$  with the ground states only, as in [3]. This approximation is indicated by the index 0. But at high temperatures, high lying levels contain a significant part of the yield, especially when they have a large spin. When they decay via  $\gamma$  emission, they contribute to the yields in eq. 1. Another problem is due to particle-unbound levels. This reduces the yields of the decaying fragments and increases the yields of daughter fragments (side-feeding) [14]. Therefore  $Tr^0$  is only an apparent temperature.

Let us examine the  $Tr^0$  values obtained with various isotope pairs listed in fig. 1,2. When  $B$  is not large ( $\approx 5$  MeV), i.e. p,d- $^6\text{Li}$ ,  $^7\text{Li}$  and  $^7\text{Li}$ ,  $^8\text{Li}$ - $^6\text{Li}$ ,  $^7\text{Li}$ , the curves increase very slowly with  $E^*/A$  and saturate at low values. Such ratios are useless. When the isotopes having the largest binding energy difference,  $^3\text{He} - \alpha$ , are involved, larger  $B$  values are obtained and  $Tr^0$  increase more with  $E^*/A$ . However the values obtained with the isotopes p,d and d,t at the numerator never exceed 6 MeV. Only  $T^0(^6\text{Li}^7\text{Li} - ^3\text{He}\alpha)$  (used by Aladin group) reaches high values, but instead of a plateau a small and gradual variation of slope is observed.

Since low values of excitation energies are reached in peripheral collisions and high values in central collisions, different collision dynamics at different impact parameters could possibly contribute to the observed behavior. To check this point, Ar + Ni data obtained at 52, 74 and 95 MeV/u were analyzed with the same method, after removing the larger part of the few fusion events present at 52 MeV/u. At the same excitation energy obtained at different impact parameters, the three  $Tr^0$  values are equal: fig. 2.

## APPARENT TEMP. FROM KINETIC ENERGY SPECTRA

Kinetic energy spectra in the QP frame were analyzed for light charged particles, since they are less sensitive to possible collective expansion. The (inverse) slope parameters  $T_s$  were obtained via the usual fits with Maxwell-Boltzmann distributions. Results for quasi-Xe nuclei

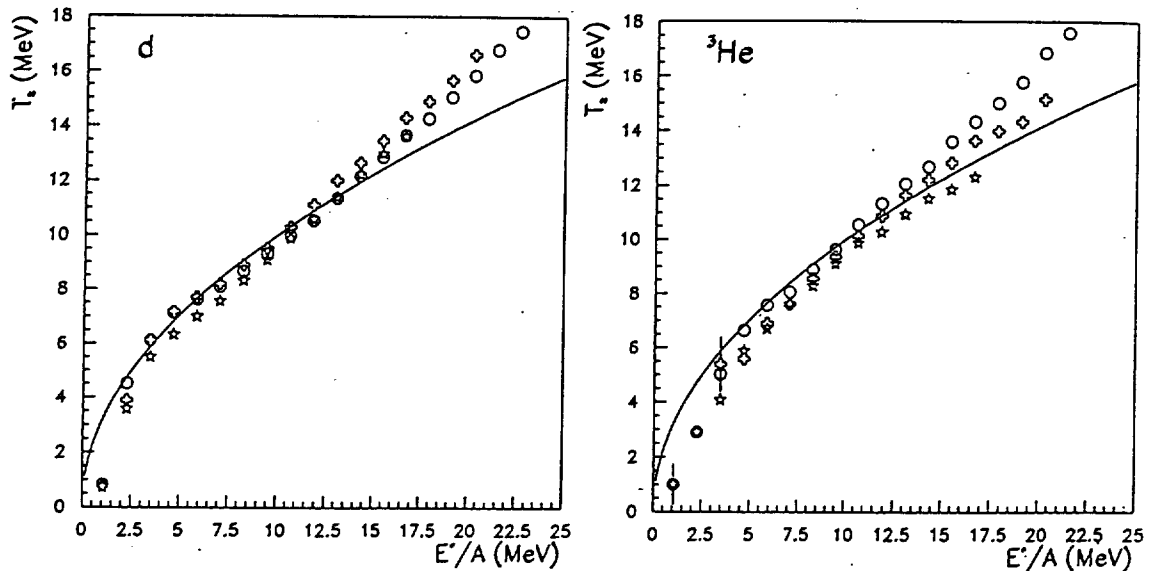


Figure 4. Same as fig. 3 for  $^{36}\text{Ar}$  at 52, 74 and 95 AMeV, for deuterons (left) and  $^3\text{He}$  (right). The symbols are the same as in fig. 2. For orientation, the Fermi gas relationship is shown with  $A/10$  (solid lines).

are shown in fig. 3.  $^3\text{He}$  slope parameters are higher than those of other light particles, which may mean they are emitted earlier, but this effect is not seen with quasi-Ar ; a specific study is in progress. The slight increase from p's to  $\alpha$ 's can be due to a small collective expansion. Each type of particle exhibits a monotonic and fast increase with  $E^*/A$ , as is also the case for quasi-Ar in Fig. 4. This figure also shows a very good agreement between the values obtained at 3 incident energies for deuterons (left panel). The same independence on incident energy is obtained for p and t. For  $^3\text{He}$  (right panel) and  $\alpha$ , differences in  $T_s$  reach 10% at high  $E^*/A$  values. This is related to the error made on the velocity of the reconstructed QP in central collisions.

## APPARENT TEMP. FROM EXCITED STATE POPULATION

The third available method is the relative population of excited states. When a nucleus is emitted from a source with a temperature  $T_{emi}$ , two levels of this nucleus separated by  $\Delta E$  are populated in proportion to  $e^{-\Delta E/T_{emi}}$  and their spins. The levels which could be identified are those which decay via emission of two charged products detected by two modules. INDRA was not designed for this purpose and only well separated levels can be identified. A detailed discussion of the methods and results will be given [18]. Here is shown only the emission temperature obtained for  $^5\text{Li}$  between the g. s. and 16.6 MeV : fig.6, bottom panel. The huge statistics needed does not allow to get narrow bins of  $E^*/A$ .  $T_{emi}(^5\text{Li})$  does not exceed 6 MeV.

## SEQUENTIAL DECAY CALCULATIONS

In order to investigate the difference between the initial temperature,  $T_{ini}$ , and the various apparent temperatures, we applied the standard evaporation model. Even if its basic

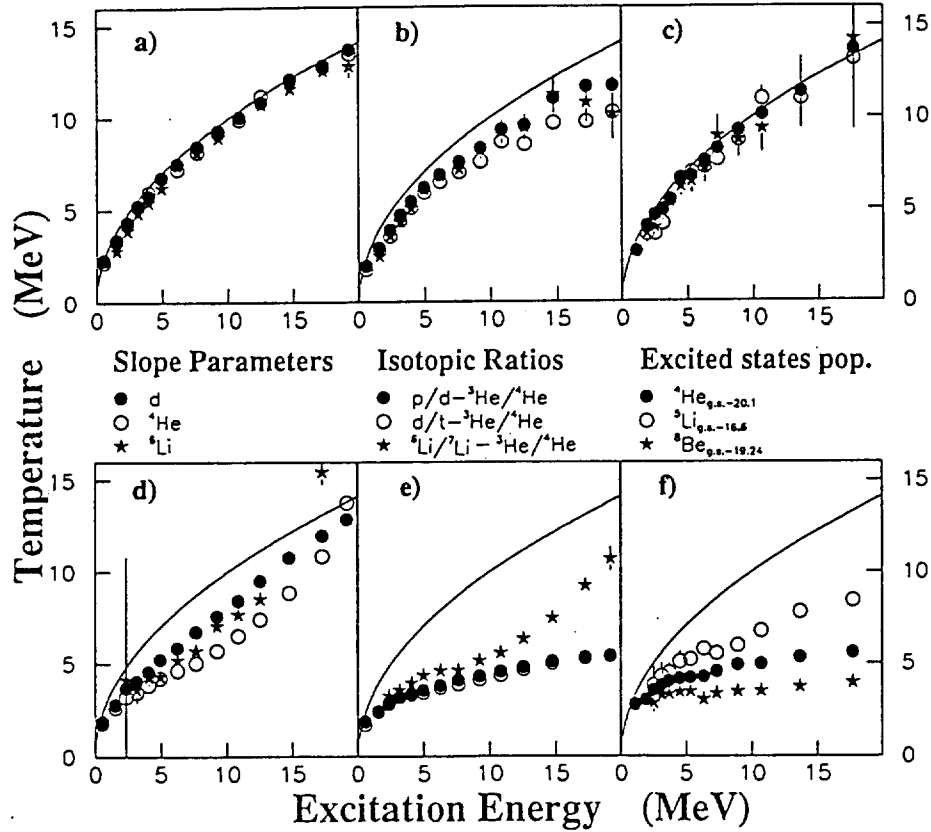


Figure 5. Sequential statistical model calculations. Solid lines: assumed initial temperature versus the excitation energy per nucleon. Points: calculated apparent temperatures obtained via 3 methods. Top panel : particles evaporated first, before decay of discrete levels. Bottom panel : particles emitted at all de-excitation steps, after decay of discrete and continuum states.

assumption (thermal equilibrium re-established between successive independent emissions) is not valid at very high  $E^*$ , it allows us to see the effects of several de-excitation steps and side-feeding. The Fermi gas relationship was assumed at all excitation energies.

Firstly, the code was stopped after first chance emission.  $T_s$  and  $T_{emi}$  have to be equal to the initial temperature : fig. 5a,c.  $Tr^0$  also should be equal, provided we take only fragments emitted in the ground state ; since excited fragments are included (as in the experiment), it is a bit lower at high  $E^*/A$ : fig. 5b. When the particle decay of discrete levels is allowed, all temperatures decrease quite moderately.

A very different situation is obtained when the full evaporation chain is studied. Detailed studies were performed by switching off or on particle decay of discrete levels, and taking into account the maximum width of these levels [21]. Fig. 5d,e,f show the final step.  $Tr^0$  values obtained with small values of  $B$  (not plotted) are almost constant with  $E^*/A$ , like experimental data (fig. 1,2). When  $B$  is large, some increase is kept, especially for <sup>6</sup>Li <sup>7</sup>Li-<sup>3</sup>He $\alpha$  which exhibits a change of slope with  $E^*$  quite similar to the data (fig. 2) and almost mimics a liquid-gas phase transition ! Even with very large  $\Delta E$  values,  $T_{emi}$  is severely reduced by side-feeding: fig. 5f. The slope parameters are much less influenced by both disturbing processes: fig. 5e.

If the decaying nucleus is thermalized, the various apparent temperatures must be reproduced with the same initial temperature,  $T_{ini}$ . The calculations in fig. 5 were made

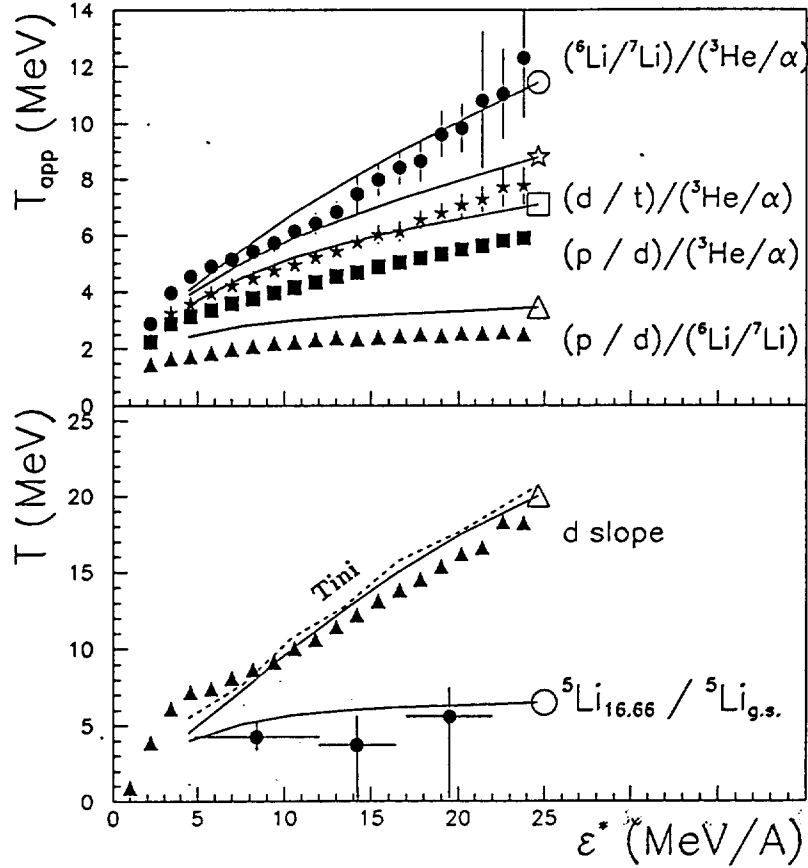


Figure 6. Extended QSM calculations compared to data. Solid symbols: experimental data; upper panel:  $Tr^0$  values; bottom panel:  $T_s$  for deuterons,  $T_{emi}$  for  ${}^5\text{Li}$  (preliminary values). Dashed line: correlation between initial temperature and excitation energy assumed in the calculation. Solid lines and open symbols : calculated apparent temperatures corresponding to the solid symbol with the same shape.

for Ar nuclei with the Fermi gas relationship and can be compared to data (fig. 2, 4 and 6).  $T_{emi}({}^5\text{Li})$  is too large, but a rather good agreement is seen with  $T^0(\text{p,d-}{}^3\text{He},\alpha)$ ,  $T^0(\text{p,d-}{}^6\text{Li},{}^7\text{Li})$  and  $T_s$  values, while a correlation assuming a plateau ( $T_{ini}$  constant for  $E^*/A = 3.6\text{-}11$  MeV, shown in [16]) clearly disagrees with most data.

## EXTENDED Q.S.M. AND INITIAL TEMPERATURES

At high  $E^*/A$ , sequential decay is not likely, so an opposite assumption was studied<sup>[22]</sup> : the emitting source is viewed as a nuclear gas in thermal and chemical equilibrium undergoing simultaneous disassembly at a given density  $\rho$  and temperature  $T$  [19].

Corrections to the ideal gas were included in the form of excluded volume effects [20]. This correction plays an important role. The excitation energy has been calculated as the total energy of the freeze-out configuration. This latter quantity has been fixed to reproduce the experimental excitation energy dependence of the measured ratio between the charge carried by light charged particles ( $Z=1,2$ ) and the total charge. This leads to a good reproduction of the charge distributions for  $E^*/A \geq 10$  MeV. The initial temperatures steadily increase from 2 to 18 MeV.

In fig. 6 the calculated  $Tr^0$  values,  $T_s$  for deuterons and  $T_{emi}({}^5\text{Li})$  are compared



to the data. The differences between the various apparent temperature are essentially due to side-feeding. These results were obtained by taking into account levels with widths  $\leq 2$  MeV (source lifetime  $\geq 100$  fm/c). The sensitivity to this parameter is shown in [16, 22]. Above  $\approx 6$  MeV per nucleon, all apparent temperatures are rather well reproduced.

## CONCLUSION

Apparent temperatures obtained from isotope ratios, kinetic energy distributions and excited state populations were determined for quasi-projectiles formed in collisions of  $^{36}\text{Ar}$  on Ni at 95, 74 and 52 MeV/u and  $^{129}\text{Xe}$  on Sn at 50 MeV/u. Nearly constant QP masses were selected over the whole range of excitation energies which reaches 24 MeV per nucleon or 13 MeV, depending on the system. Two types of calculations show that apparent temperatures based on isotope yield ratios or excited level populations are very sensitive to the role of high energy resonances and that the initial temperature values are subject to a large uncertainty. At excitation energies above 10 MeV per nucleon, these apparent temperatures are much lower than the initial temperatures. The kinetic temperatures (slope parameters) of light particles keep a good memory of the initial temperature, provided no large collective motion is present. No evidence is found for a plateau followed by a rise (first order liquid-gas phase transition) in the relationship between  $T$  and  $E^*/A$ , neither in the experimental data (apparent temperatures), nor in the initial temperatures obtained via calculations. The initial temperature grows steadily with excitation energy on the whole range of excitation energies. Up to  $\approx 10$  MeV per nucleon, this increase is very close to that of a Fermi gas. At higher excitation energies, multifragmentation sets in and the temperature increases faster with excitation energy. Instead of a rather sharp transition, a gradual evolution is found.

## REFERENCES

1. R. Wada et al., Phys. Rev. C **39** (1989) 497 and references therein.
2. J. Pochodzalla et al., Phys. Rev. C **35** (1987) 1695 and references therein.
3. J. Pochodzalla et al., Phys. Rev. Lett. **75** (1995) 1040.
4. J.C. Steckmeyer et al., Phys. Rev. Lett. **76** (1996) 4895.
5. J. Péter et al., Nucl. Phys. A **593** (1995) 95.
6. S. Albergo et al, Nuovo Cimento A **89** (1985) 1.
7. J. Bondorf et al, Nucl. Phys. A **444** (1985) 460, A **448** (1986) 753
8. J. A. Hauger et al., Phys. Rev Lett. **77** (1996) 235.
9. D. H. E. Gross et al., Phys. Lett. B **200** (1988) 397.
10. Sa B.-H., Nucl. Phys. A **499** (1989) 480.
11. L. G. Moretto et al., Phys. Rev. Lett. **76** (1996) 2822
12. X. Campi et al., Phys. Lett. B **385** (1996) 1
13. J. Natowitz et al., Phys. Rev. C **52** (1995) R2322
14. M. B. Tsang et al., Phys. Rev. C **53** (1996) R1057
15. H. F. Xi et al., preprint MSUCL-1040 (1996)
16. Y.G. Ma et al., Phys. Lett. B **390** (1997) 41
17. M.F. Rivet et al., Phys.Lett. B **388** (1996) 219. B. Borderie et al., Phys.Lett. B **388** (1996) 224
18. M. Assenard, Ph. D. Thesis Nantes, 1997.
19. A.Z. Mekjan, Phys. Rev. C **17** (1978) 1051
20. R. K. Tripathi and L.W. Townsend Phys. Rev. C **50** (1994) R7
21. A. Siwek et al., Proc. XXXI Zakopane School, Poland (1996)
22. F. Gulminelli and D. Durand, preprint LPCC 96-11, Nucl. Phys. A (accepted).